New Fréedericksz thresholds in three dimensions

Axel Kilian*
Institut für Theoretische Physik, Technische Universität Berlin, Hardenbergstrasse 36, D-12046 Berlin, Germany
(Received 12 November 1993; revised manuscript received 4 May 1994)

This work was inspired by a paper of Lonberg and Meyer [Phys. Rev. Lett. **55**, 718 (1985)], who observed a Fréedericksz threshold different from the usual one, $U_{\mathrm{Fred}}=\pi\sqrt{K_1/\Delta\varepsilon}$, which results from a one-dimensional (1D) stability analysis and which underlies measurement techniques of the Frank elastic constant K_1. The new threshold occurs in polymer constituent nematic liquid crystals, which possess, compared to the usual low-molecular-weight nematic mixtures, an unusually large ratio of K_1/K_2. It is accompanied by a periodic splay-twist distortion parallel to the director field. The stability estimations given by Lonberg and Meyer were later confirmed by Cohen and Luskin [in *Nematics: Mathematical and Physical Aspects,* Vol. 332 of *NATO Advanced Study Institute, Series C: Mathematical and Physical Sciences,* edited by J. F. Coron, F. Helein, and J. M. Ghidaglia (Kluwer, Dordrecht, 1991), p. 261], who used a new variation method to determine "weak stability." Due to the fundamental role of Fréedericksz transitions not only in measurement techniques, but also in the operation of many electro-optical devices, I found that the problem of stability in 3D deserves systematic investigation. Since there is not much hope of obtaining analytical solutions of the respective Euler-Lagrange equations in 3D, I programmed a scheme that simulates the measurement process of elastic constants at different geometries. As a result, I could first reconfirm the known effect, and second, predict a new instability mode that should occur in nematic liquid crystals with a negative dielectric anisotropy subjected to homeotropic anchoring. Analytical expressions for the 3D threshold values support the numerical results.

PACS number(s): 64.70.Md, 02.70.Bf

I. INTRODUCTION

There are a variety of second-order phase transitions—so-called Fréedericksz effects—which accompany the operation of virtually all electro-optical devices that use nematic liquid crystals; those effects are also very useful, if not necessary, for the measurement of the elastic constants. So far, the one-dimensional (1D) calculations on which the stability analyses are based agreed perfectly in general with experiment. For a summary of the various geometries and the respective threshold values, see the Appendix.

However, there is one exception, discovered by Meyer in 1985: When he examined a new high-molecular-weight nematic, he found a periodic splay-twist distortion that appeared at the Fréedericksz threshold instead of the usual pure splay. This "new ground state" occurred at a lower field strength than predicted by Eq. (19). The key feature of the new material was an unusually high ratio of K_1/K_2 as a consequence of the length-to-width-ratio of the molecules, which was of the order of 70.

The new effect can qualitatively be understood as follows: Since the splay instability is degenerate (like any bifurcation), it can tilt in one direction at one point, and in the other direction at another point. In between, a twist distortion is generated (see Fig. 1). If the twist elastic constant, K_2 is small enough, this mode is energetically preferred to the usual instability mode, because it avoids splay.

For a quantitative understanding, a pair of two-dimensional (2D) equations (Euler-Lagrange equations of the Frank energy) would have to be solved, which the au-

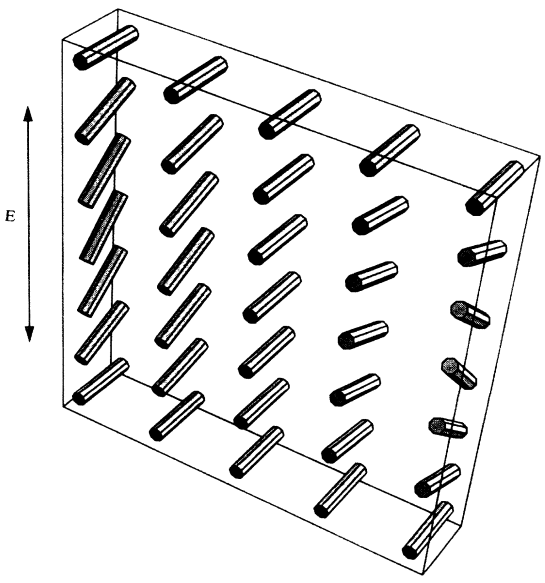

FIG. 1. Periodic bend-splay distortion that occurs for large ratios of K_1/K_2.

*Electronic address: axel@siggi.physik.tu-berlin.de

thors of [1,2] could only do numerically. Second they found, first that the periodic bend-splay distortion should occur whenever $K_1/K_2 > 3.3$ (this number is actually very close to the exact analytical value found by Oldano [3]). Second, they found that the in-plane wave vector of the distortion should somehow increase close to the critical ratio. The latter could not be confirmed in experiment.

II. BASIC EQUATIONS AND THE NUMERICAL ALGORITHM

The anisotropic part of the free energy of a nematic subjected to a prescribed electric field is

$$f = f_{\text{el}} + f_{\text{chiral}} + f_{\text{field}} , \tag{1}$$

where

$$f_{\text{el}} = \frac{K_1}{2}(\text{div}\mathbf{n})^2 + \frac{K_2}{2}(\mathbf{n}\cdot\nabla\times\mathbf{n})^2 + \frac{K_3}{2}(\mathbf{n}\times\text{rot}\mathbf{n})^2 , \tag{2}$$

$$f_{\text{field}} = \frac{\Delta\varepsilon}{2}(\mathbf{n}\cdot\mathbf{E})^2 , \tag{3}$$

and

$$f_{\text{chiral}} = \frac{2\pi K_2}{p_0}\mathbf{n}\cdot\text{rot}\mathbf{n} ; \tag{4}$$

p_0 is the intrinsic cholesteric pitch. In Eq. (3), a prescribed field is assumed. Usually a nematic cell, however, operates with a prescribed voltage, and the field depends on the director configuration. For 1D, Deuling has found an analytic solution [4]. Since in this paper only very small distortions of a constant director field are considered, the difference between prescribed field and prescribed voltage is negligible.

For numerical purposes, the equivalent form [5]

$$f_{\text{el}} = \frac{K_1 - K_2}{2}(\nabla_\alpha n_\alpha)^2 + \frac{K_2}{2}(\nabla_\alpha n_\beta)(\nabla_\alpha n_\beta) + \frac{K_3 - K_2}{2} n_\alpha n_\beta (\nabla_\alpha n_\gamma)(\nabla_\beta n_\gamma) \tag{5}$$

is more suitable and differs from Eq. (2) only by a surface term. In order to simulate a measurement process of an elastic constant, a dynamic equation is necessary. It is deduced from Eq. (5) by variational derivative, i.e.,

$$\dot{n} = \alpha\left[\frac{\delta f}{\delta n} + \lambda n\right] , \tag{6}$$

where α is a proportionality factor and λn stems from the variation of the constraint $n_\mu n_\mu = 1$, λ being the Lagrange multiplier. By comparison with a dynamic equation for the alignment tensor which was formulated by Hess in 1975 [6], it is found that

$$\alpha = -\frac{1}{\gamma_1} , \tag{7}$$

γ_1 being the rotational viscosity. Inserting Eqs. (1) and (7) in Eq. (6) yields the explicit form

$$\gamma_1 \dot{n}_\alpha = (K_2 - K_1) g_\alpha^{(1)} - K_2 g_\alpha^{(2)} + (K_2 - K_3) g_\alpha^{(3)} + g_\alpha^{(4)} + \frac{4\pi K_2}{p_0} g_\alpha^{(5)} , \tag{8}$$

where

$$g_\alpha^{(1)} = \nabla_\alpha \nabla_\beta n_\beta , \tag{9}$$

$$g_\alpha^{(2)} = \nabla_\beta \nabla_\beta n_\alpha , \tag{10}$$

$$g_\alpha^{(3)} = (\nabla_\alpha n_\beta - \nabla_\beta n_\alpha) n_\gamma \nabla_\gamma n_\beta - \nabla_\beta n_\beta n_\gamma \nabla_\gamma n_\alpha - \nabla_\beta n_\gamma \nabla_\beta \nabla_\gamma n_\alpha , \tag{11}$$

$$g_\alpha^{(4)} = \Delta\varepsilon E^2 n_z , \tag{12}$$

and

$$g_\alpha^{(5)} = \varepsilon_{\alpha\beta\gamma}\nabla_\beta n_\gamma . \tag{13}$$

The Lagrange multiplier term in Eq. (6) is omitted, and, instead, the new director at each grid point is divided by its length. This equivalent procedure is less complicated, and numerically more stable. The field term in Eq. (12) has been specialized to an electric field pointing in the z direction, and $\varepsilon_{\alpha\beta\gamma}$ in Eq. (13) is the total antisymmetric isotropic tensor of rank 3. Upon discretizing Eq. (8) on a rectangular mesh using the usual finite-difference methods, a numerical algorithm is obtained which simulates the relaxation of a nematic confined to a rectangular box. A more detailed example of this procedure can be found in [7]. The director field at the boundary is prescribed (rigid anchoring). The maximum numerically stable time step has been chosen; it depends on the material coefficients, and on the field strength. The order of magnitude was

$$0.01 < \frac{\Delta t}{\left[\frac{\gamma_1}{K_2}(\Delta x)^2\right]} < 0.15 . \tag{14}$$

Finally, it is important to apply small "fluctuations" to

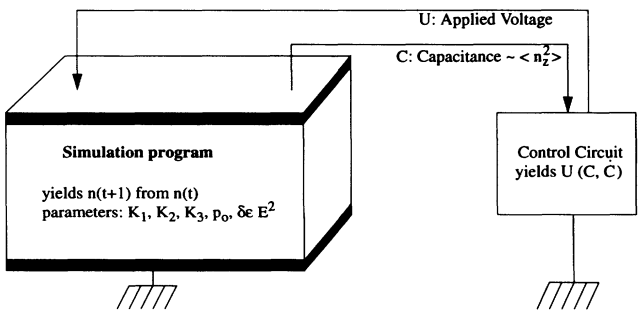

FIG. 2. Programming scheme to simulate the measurement of elastic constants for different geometries in 3D.

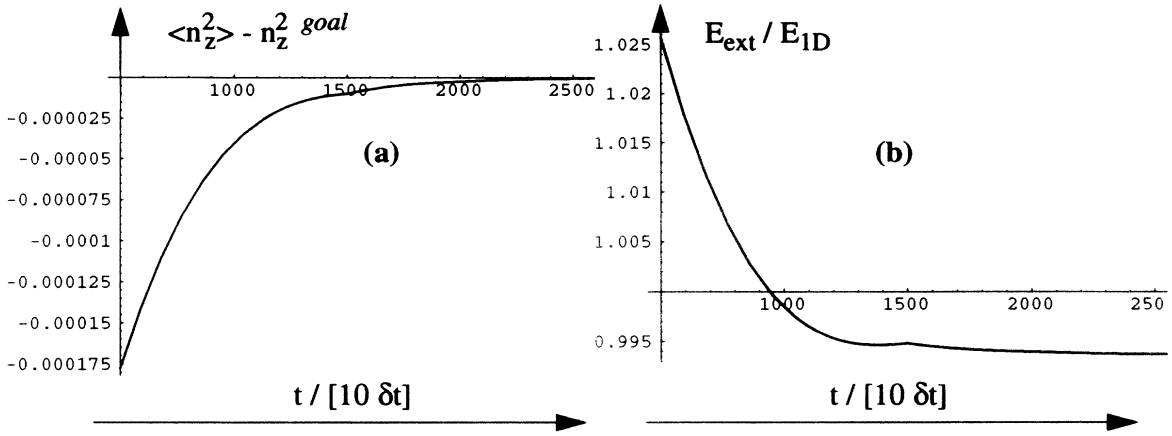

FIG. 3. Dynamics of the automatic "threshold finder."

the director field, so that any distortion mode can be found. This has been done by adding Gauss distributed random numbers to the director components. The expectation value is typically of the order 10^{-5} or smaller. Due to the Gaussian distribution function, the perturbation is isotropic. It should be mentioned that these perturbations are different from the real thermal fluctuations; they help, however, like the real thermal fluctuations, to avoid metastable director configurations.

In principle, the simulated measurement of the Fréedericksz thresholds could be done with this program "manually," that is, one could try and search for the value of the field strength at which the mean value $\langle n_z \rangle$ (in equilibrium) matches a small prescribed number, typically of the order of 10^{-3}. This, however, turned out to be impracticable due to the critical slowing down near the threshold. Actually, in real life it can take a whole day to determine a Fréedericksz threshold. In order to speed up the procedure, I wrote a program that adjusts the field strength during the relaxation, that is, in nonequilibrium. It will be described in some detail below, because it might also be useful in real experiments (see Fig. 2). The basic algorithm is

$$E^{\text{new}} = E e^{-(\varphi - \varphi_{\text{goal}}/\tau_1 + \dot{\varphi}/\tau_2)} . \tag{15}$$

Here, φ denotes $\langle n_z \rangle$ (proportional to the anisotropic part of the capacitance), and τ_1 and τ_2 are numbers typically of the order $\frac{1}{50}$ and $\frac{1}{3000}$, respectively. In order to avoid an increasing oscillation, it is necessary to take the

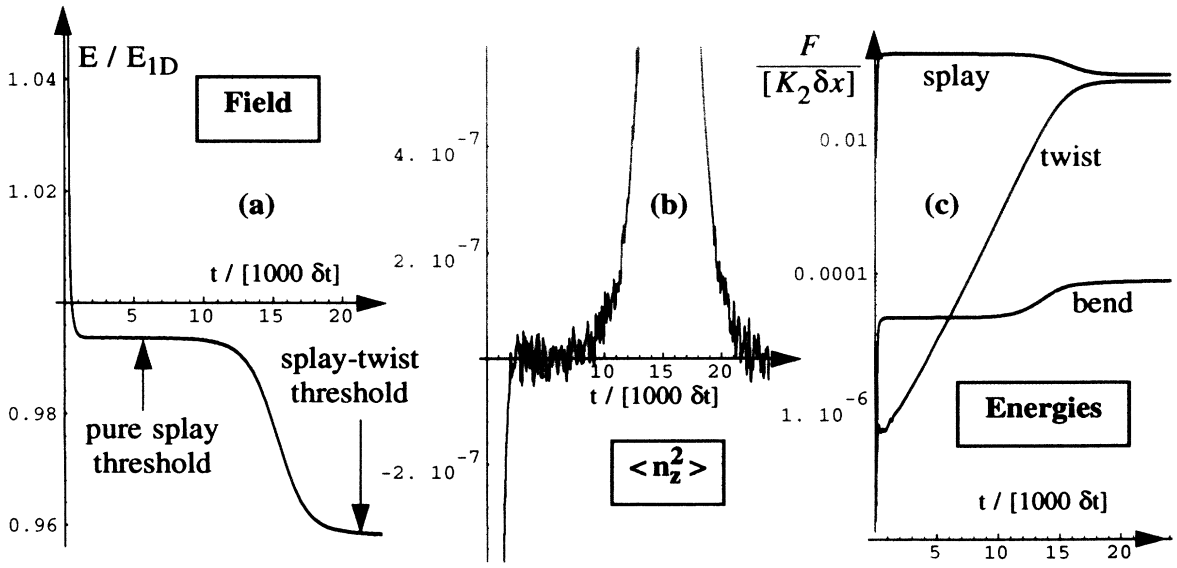

FIG. 4. Operation of the threshold finder for a nematic with a splay-twist ratio $K_1/K_2 = 5$.

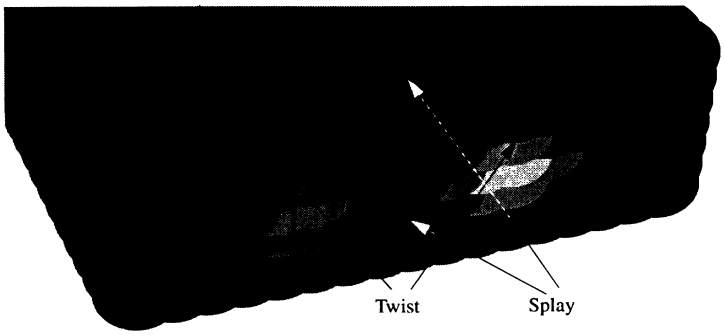

FIG. 5. Spatial distribution of the elastic energies for the splay-twist distortion occurring at a ratio $K_1/K_2=5$.

time derivative of φ into account, with much more emphasis than on φ itself. In Fig. 3, a simulated relaxation based on Eq. (15) is depicted. It corresponds to a 2D simulation area of 99×9 grid points and Fréedericksz geometry. The 1D threshold was found in less than 2500 time steps. For a cell of 10 μm filled with MBBA, this would correspond to 17 s [cf. Eq. (14)], at room temperature, when $K_2=4\times10^{-12}$ N and $\gamma_1=0.77$ Pa s. The accuracy obtained was better than 0.6%, which is very good for a cell with only 9 grid points in diameter. Random perturbations of magnitude 5×10^{-5} were applied.

III. FRÉEDERICKSZ GEOMETRY

This chapter is a review of Meyer's periodic splay-twist distortion, as described in the Introduction. It serves mainly as a test of the program.

For the simulations presented in this chapter, free boundary conditions have been used. That means that the lateral boundaries (but not the top and bottom layers) exert no constraints on the director field. Mathematically, this corresponds to the condition that the gradient of the director field in the direction of the boundary layer normal vanishes. In the program, this has been accomplished by setting a directors in the boundary layers equal to its nearest neighbors in the bulk.

I would like to begin with an example, and proceed then more systematically. The example is a nematic with a splay-twist ratio $K_1/K_2=5$. In Fig. 4, the dynamics of the approach toward the threshold is shown. Actually, two thresholds are approached: first, the usual 1D threshold, and, later, another threshold, which is lower.

The whole process takes 24 000 time steps, which corresponds to almost 3 min even for a cell of only 10 μm filled with MBBA. The usual 1D threshold is found in a few seconds. Then, for a minute, nothing seems to happen. Suddenly, the "capacitance" $\langle n_z^2\rangle$ jumps to a higher value, which is immediately compensated by decreasing the applied voltage. A new equilibrium is approached for the decreased voltage. In the present case, the lower three-dimensional (3D) threshold differs from the 1D threshold only by 5%. As can be seen in Fig. 4(c), a twist distortion which evolves very slowly is the reason for that unusual behavior.

The spatial distribution of the elastic energies is depicted in Fig. 5. The in-plane distance between two neighboring twist regimes is here of the order of the cell thick-

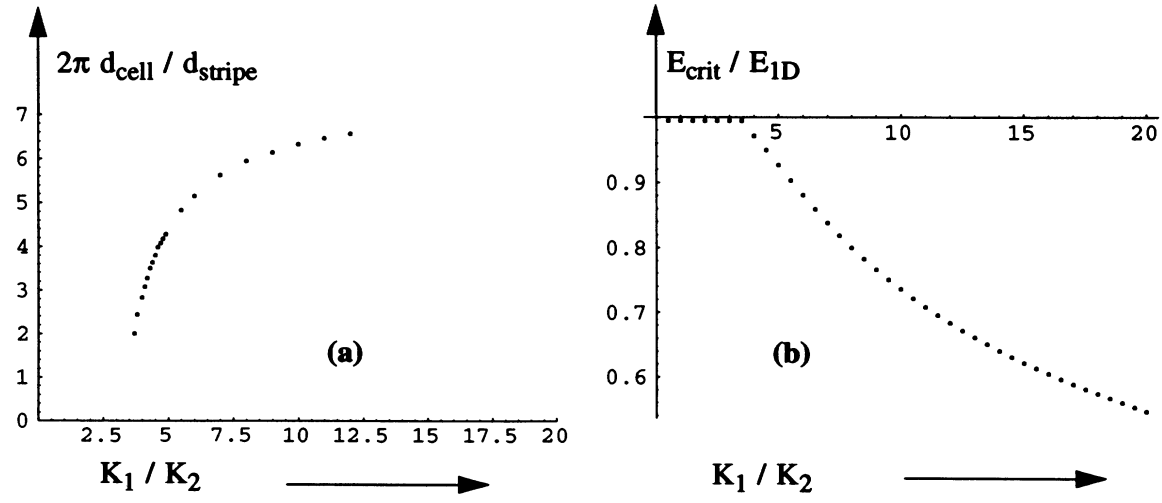

FIG. 6. (a) Dependence of the inverse stripe distance (in-plane wave vector) on K_1/K_2. For large values of K_1/K_2, the stripe distance approaches a value close to the cell thickness, whereas there is a minimum value R_{crit} for K_1/K_2, where the stripe distance diverges. (b) Dependence of the threshold on K_1/K_2. The small deviation of the 1D threshold from unity is due to a discretization error of 0.7%, which is very small for a cell with only 7 grid points in diameter.

ness.

Next, the dependence of the threshold on K_1/K_2 and on the stripe distance is investigated. This is done by a loop over K_1/K_2 from 1 to 20. In Fig. 6(a), the in-plane wave vector, and in Fig. 6(b), $E_{\text{threshold}}/E_{\text{1D}}$ are plotted both as a function of K_1/K_2.

The data for the latter plot were obtained by a discrete Fourier transform of the director field, and subsequent smoothing with spline functions of the order of 9. As a consequence of this complicated procedure, this part of the simulation might be less accurate than the rest. Nevertheless, the Figure indicates correctly that the in-plane wave vector becomes zero (the stripe distance diverges) somewhere around 3.3.

According to Fig. 6(b), the critical ratio of K_1/K_2 seems to be somewhere between 3.5 and 4, whereas the correct value should be ~ 3.300. This small deviation has the following origin: Since the splay-twist instability mode as a function of K_1/K_2 exhibits a second-order phase transition, there is a critical slowing down. As a consequence, the data which are close to the critical ratio are less accurate than the rest, because they are not quite in equilibrium (all data were obtained by applying a fixed number of 400 000 time steps to the liquid crystal). In the simulations, no splay-twist distortion arose below a value of $K_1/K_2=3.7$, probably due to both the limited simulation area and the limited time. In order to come closer to the diverging point, a larger simulation area and more time steps would have been needed. For the present purpose, which is mainly a test of the program, this did not appear to be necessary.

IV. HOMEOTROPIC GEOMETRY

This chapter contains in its first part the result that an anticipated effect does not exist. The second part presents, as a prediction, a new instability mode which should occur for nematics with a negative dielectric anisotropy and a ratio of K_1/K_2 which is above a certain threshold value.

A. Free boundary conditions

The main result for this setup is that there is no difference between 1D and 3D, that is, the usual threshold as given by Eq. (20) is found (again, with a small discretization error of 0.6%). I tried ratios K_3/K_2 up to 100, at which value the program collapsed due to numerical instabilities.

At first glance, this is surprising because one would expect an effect analogous to the one described in Sec. III (i.e., pure bend would be released by a periodic bend-twist structure). This simply did not happen in my simulations. By exerting an artificial constraint on the director field I checked that the cause was not the additional degree of freedom occurring in the homeotropic geometry. Looking at the problem more closely, I found that the differential equations are quite dissimilar, although they lead to equivalent distortion modes and Fréedericksz thresholds. Actually, even the Euler-Lagrange equations in 1D are quite different (cf. [8] and [9]).

B. Rigid anchoring

Here, a rectangular box, and also a spherocylinder, both with fixed boundary conditions at all boundary layers, are examined. Actually, the shape is not as important as the fact that now the director field at the lateral boundary is fixed. Although this case is analytically easier to handle, there is no one-to-one mapping to an experimental situation. Physical situations which approximately meet this model are (1) a single pixel embedded in a homeotropic environment and (2) laser-induced Fréedericksz transitions, where also only a very small region of the sample is addressed by a laser beam.

Simulating this setup, I found that for ratios of K_1/K_2 above a certain threshold value, a new type of distortion mode occurs, which comes along with a lower threshold. This chapter proceeds as follows: After introducing the new effect by a specific example, the two different instability modes will be examined more quantitatively.

In Fig. 7, the equilibrium director fields obtained with the threshold finder for two different values of K_1/K_2 are depicted. Since the threshold finder yields director fields with very small distortions, the x and y components of the director field have been amplified by a factor of 10.

The left configuration belongs to a ratio of $K_1/K_2=1$. As can be seen, the director field is just tilted. If the lateral edges are of equal length, or if $K_1=K_2$, the director can tilt in any direction. In contrast to the 1D instability mode, this distortion is not a pure bend, but contains also splay (here at the top and bottom of the Figure) and twist (here at the left and right sides of the Figure). Another effect of the finite lateral size of the box is an increase of the Fréedericksz threshold, compared to the 1D threshold given by Eq. (20). Both simulation areas consisted of only $7\times7\times7$ grid points, which is a resolution too low for quantitative results, but good enough to demonstrate the effect in principle.

From semianalytical calculations to be presented in Secs. 2 and 3 of the Appendix analytical expressions have

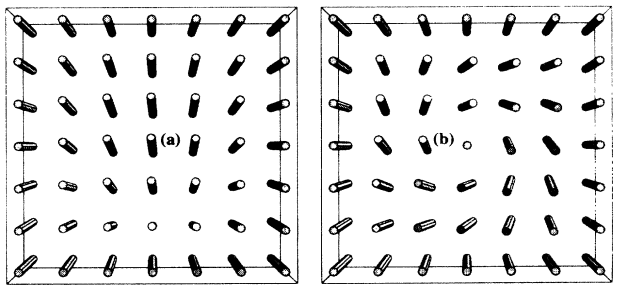

FIG. 7. Top view of the director fields slightly above the threshold (only the center layer is depicted). The small distortion has been amplified by a factor of 10. (a) At $K_1/K_2=1$, the director field exhibits the usual bend-twist-splay instability mode (BTS), that is, it may tilt in one (arbitrary) direction. (b) At $K_1/K_2=7$, the director field is rotationally symmetric, and any radius vector coincides with a twist axis, so that a double-twist distortion (DT) occurs.

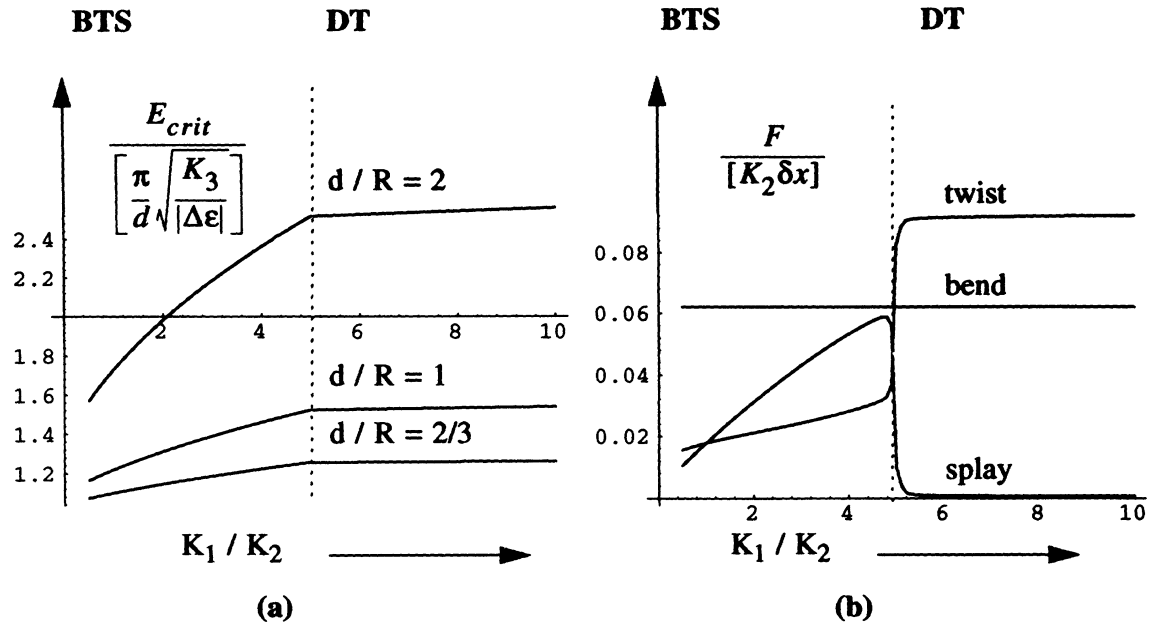

FIG. 8. (a) Dependence of the Fréedericksz threshold on K_1/K_2. Above a critical value of $K_1/K_2 \sim 5$, the threshold should theoretically stay constant. (b) The elastic energies in an equilibrium state slightly above the Fréedericksz threshold as a function of K_1/K_2. When the director field transforms from the BTS to the DT configuration, splay is replaced by twist energy.

been obtained for the Fréedericksz thresholds at which the above distortions occur. They are

$$E_{\text{crit}}^{\text{BTS}} = \frac{\pi}{d}\left[\frac{K_3+(K_1+K_2)\hat{w}^{-2}}{|\Delta\varepsilon|}\right]^{1/2}, \tag{16}$$

where a nematic confined to the rectangular box

$$[-w/2,w/2]\times[-w/2,w/2]\times[-d/2,d/2],$$

is assumed and $\hat{w}$ is the (dimensionless) lateral size in units of the cell gap d. When $\hat{w}$ is large, the 1D threshold, Eq. (20), is approach.

The double-twist threshold

$$E_{\text{crit}}^{\text{DT}} = \left[\left(\frac{\pi}{d}\right)^2\frac{K_3}{|\Delta\varepsilon|}+\left(\frac{B_0}{R}\right)^2\frac{K_2}{|\Delta\varepsilon|}\right]^{1/2} \tag{17}$$

is based on the assumption that the nematic is confined to a spherocylinder of height d and radius R; $B_0 \sim 3.831$ is the first zero of the Bessel function $J_1(x)$.

Since $E_{\text{crit}}^{\text{BTS}}$ depends on K_1, whereas $E_{\text{crit}}^{\text{DT}}$ does not, there is a crossover at a critical ratio of K_1/K_2, above which the double-twist instability mode is energetically preferred. This value is found to be

$$K_{1/2}^{\text{crit}} \sim 4.95 . \tag{18}$$

Again, it has been assumed that the cavity shape is of minor influence, so that $w=2R$. Since Eq. (18) is based on some approximations, it is compared to numerical solutions. Some quantitative numerical results are displayed below.

Figure 8(a) shows that the critical ratio of $K_1/K_2 \sim 5$ is well reproduced. For $K_1/K_2=1$, Eq. (16) matches the numerically obtained threshold well. In particular, for only $7\times7\times7$ grid points, $E_{\text{num}}/E_{\text{ana}}=0.988$. For $K_1/K_2=4$, $E_{\text{num}}/E_{\text{ana}}=0.96$, although the simulation area was $19\times19\times19$ grid points. This deviation reflects that Eq. (16) is strictly valid only if $K_1=K_2$, but indicates at the same time that it is a good approximation.

Comparing the double twist (DT) threshold to Eq. (17), one sees immediately that the numerically obtained threshold as a function of K_1 is not constant; it has a small but finite slope. The accuracy was still better than 3% for the largest simulation area ($31\times31\times11$ grid points, corresponding to $d/R=\frac{2}{3}$).

In Fig. 8(b), the assumption that the double-twist instability mode has no splay at all (this assumption is used in the stability analysis presented in Sec. 3 of the Appendix) is nicely confirmed. The quasidiscontinuity indicates that the instability mode as a function of the control parameter K_1/K_2 undergoes a first-order phase transition.

V. CHOLESTERICS

The same double-twist instability as described in Sec. IV B 4.2 can also occur in chiral nematics. It exists, however, only for low chirality (the chirality inhibits the double-twist instability mode). Low chirality means here that the pitch should be as long as necessary to reduce the critical field, compared to an untwisted nematic, by not more than 10–20 % [cf. Eq. (20)].

As already mentioned at the beginning of Sec. IV B, the mathematical construct of rigid anchoring at the lateral boundaries is not canonically relatable to a physical device or setup. In order to overcome this potential drawback and to be more realistic, I simulated a pixel. A

pixel (picture element) is the smallest part of a display that can be addressed. The setup of a chiral nematic with a negative dielectric anisotropy subjected to homeotropic anchoring has been used in a dichroic display, which requires no polarizers [10]. This time I did not use the "threshold finder" described above, but used a constant field 10% above the Freedericksz threshold. The field was applied only in a center region. In that way, the rim region serves as the homeotropic environment of the pixel. The specific parameters were $K_1/K_2=7$, $K_3/K_2=1$, and p_0 such that the intrinsic rotation per lattice unit was 0.07 rad. The simulation area was $51\times11\times11$ grid points, which corresponds to a small pixel of 0.1×0.1 mm, if the cell gap is 20 μm.

As a result, I could switch the cell within the rotationally symmetric DT mode between a weakly tilted off state and a strongly tilted on state. In order to achieve reasonable switching times, a small holding voltage is needed which preserves the small DT instability. The rotationally symmetric director field might be interesting for applications which require a wide viewing angle. Since no fundamentaly new features arose in this simulation, I simply report that the DT instability mode should also occur in cholesterics.

VI. CONCLUSIONS

A known 3D effect has been reconfirmed, which may be considered a test of the program. A systematic investigation of various geometries indicates the following.

(1) An equivalent to the periodic splay-bend instability, namely, a periodic bend-twist instability does *not* occur in nematics with negative dielectric anisotropy and perpendicular anchoring, as might be expected.

(2) Instead, a rotationally symmetric instability mode of the director field is energetically preferred when the ratio of K_1/K_2 exceeds a critical value of ~5. This numerically obtained result is confirmed by linear stability analyses.

(3) The same effect can also occur in cholesterics with weak chirality. As a possible application, the operation of an existing device [10] would considerably be altered and, very likely, improved. For this, new material with a sufficiently high ratio of K_1/K_2 and, at the same time, a reasonably low rotational viscosity γ_1 will have to be synthesized.

ACKNOWLEDGMENT

The financial support of the Deutsche Forschungsgemeinschaft via the Sonderforschungsbereich "Anisotrope Fluide" is gratefully acknowledged.

APPENDIX

1. Review: 1D Fréedericksz thresholds

Fréedericks transitions can occur when an electric or a magnetic field is applied which is perpendicular to the director field. If the anchoring at the top is parallel to that at the bottom, the respective distortion modes are pure bend, twist, or splay distortions. In any other case, mixed types occur. The various geometries and the respective distortion modes are depicted in Fig. 9.

The corresponding critical fields for all of the depicted geometries are covered by three formulas.

(1) Planar anchoring at the surfaces, which may be twisted by an angle β_T, and a positive dielectric anisotropy:

$$E_{\rm thr}^{\rm par}=E_0\left\{1+\frac{K_3-2K_2}{K_1}\left[\frac{\beta_T}{\pi}\right]^2+\frac{4dK_2\beta_T}{p_0K_1\pi}\right\}^{1/2},$$

where

$$E_0=\frac{\pi}{d}\left[\frac{K_1}{\varepsilon_0\Delta\varepsilon}\right]^{1/2}, \tag{A1}$$

d is the cell diameter, and p_0 the intrinsic pitch of a chiral nematic. This formula was first published by Berreman [8].

(2) Perpendicular anchoring at the surfaces, and a negative dielectric anisotropy:

$$E_{\rm thr}^{\rm per}=\frac{\pi}{d}\left\{\frac{-K_3}{\varepsilon_0\Delta\varepsilon}\left[1-\left[\frac{2dK_2}{p_0K_3}\right]^2\right]\right\}^{1/2}, \tag{A2}$$

as was found by Greubel [9].

(3) The threshold for the "twist" geometry in Fig. 9 is given by

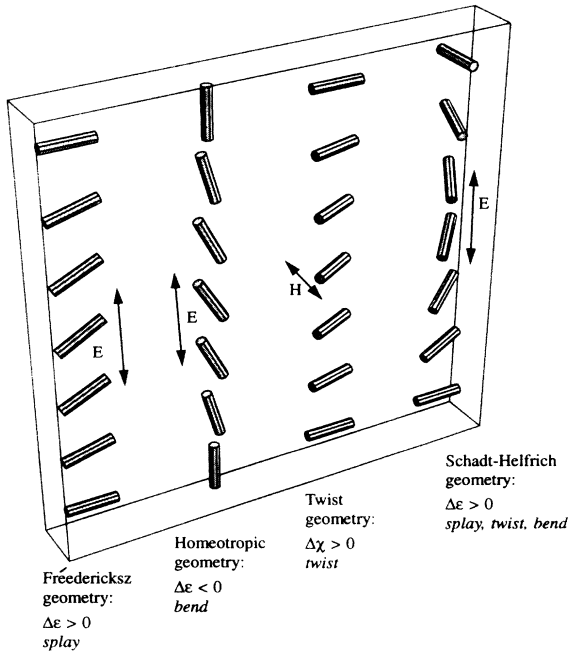

FIG. 9. Distortion modes of some geometries which exhibit Fréedericksz transitions. The double arrow indicates the direction of the applied field.

$$H_{\mathrm{thr}}^{\mathrm{twist}}=\frac{\pi}{d}\left[\frac{K_2}{\Delta\chi}\right]^{1/2} . \tag{A3}$$

All results employ the assumption that the director field is homogeneous in the planes parallel to the walls.

2. Derivation of the 3D Fréedericksz threshold for the bend-twist-splay instability

The instability mode on which the following analytical calculation is based was obtained by inspection of the simulated director field. It is found that for $K_1=K_2$, the director field of a nematic confined to the rectangular box is very well fitted by

$$n=\begin{bmatrix}\cos\vartheta\cos\varphi\\ \cos\vartheta\sin\varphi\\ \sin\vartheta\end{bmatrix} , \tag{A4}$$

with

$$\vartheta(x,y,z)=a\cos\frac{\pi x}{d_x}\cos\frac{\pi y}{d_y}\cos\frac{\pi z}{d} \quad \text{and} \quad \varphi=\text{const} . \tag{A5}$$

Consequently, we have homeotropic anchoring at the boundaries; a is a small number. As there is no approximation that is at the same time more precise and still simple enough, this distortion mode is also used for $K_1\neq K_2$. The resulting error has already been discussed in Sec. IV B. The region of the rectangular box is

$$A_{\mathrm{box}}=\left[-\frac{d_x}{2},\frac{d_x}{2}\right]\times\left[-\frac{d_y}{2},\frac{d_y}{2}\right]\times\left[-\frac{d}{2},\frac{d}{2}\right] . \tag{A6}$$

With this ansatz, the energy density, Eq. (2), plus Eq. (3) is specified. Since only small distortions of the constant off-field equilibrium state are considered, a Taylor expansion with respect to a is appropriate:

$$f^{\mathrm{Taylor}}=f_{\mathrm{bend}}^{\mathrm{Taylor}}+f_{\mathrm{twist}}^{\mathrm{Taylor}}+f_{\mathrm{splay}}^{\mathrm{Taylor}}+f_{\mathrm{field}}^{\mathrm{Taylor}} , \tag{A7}$$

where

$$f_{\mathrm{bend}}^{\mathrm{Taylor}}=\frac{a^2\pi^2K_{11}}{2}\left[\frac{\cos\varphi\cos\frac{\pi y}{d_y}\cos\frac{\pi z}{d}\sin\frac{\pi x}{d_x}}{d_x}+\frac{\cos\frac{\pi x}{d_x}\cos\frac{\pi z}{d}\sin\varphi\sin\frac{\pi y}{d_y}}{d_y}\right]^2 , \tag{A8}$$

$$f_{\mathrm{twist}}^{\mathrm{Taylor}}=\frac{a^2\pi^2K_{22}}{2}\left[\frac{\cos\varphi\cos\frac{\pi x}{d_x}\cos\frac{\pi z}{d}\sin\frac{\pi y}{d_y}}{d_y}-\frac{\cos\frac{\pi y}{d_y}\cos\frac{\pi z}{d}\sin\varphi\sin\frac{\pi x}{d_x}}{d_x}\right]^2 , \tag{A9}$$

$$f_{\mathrm{splay}}^{\mathrm{Taylor}}=\frac{a^2\pi^2K_{33}}{2}\left[\frac{\cos\frac{\pi x}{d_x}\cos\frac{\pi y}{d_y}\sin\frac{\pi z}{d}}{d}\right]^2 , \tag{A10}$$

and

$$f_{\mathrm{field}}^{\mathrm{Taylor}}=\frac{\Delta\varepsilon E^2}{2}\left[\left[\frac{a^2\cos\frac{\pi x}{d_x}\cos\frac{\pi y}{d_y}\sin\frac{\pi z}{d}}{d}\right]^2-1\right] . \tag{A11}$$

Here, $-\Delta\varepsilon E^2/2$ is the free energy density of the undistorted homeotropic state. The remainder in Eq. (29) is the difference between the distorted and the undistorted state. Integration yields the total energy difference between the distorted and the undistorted state:

$$\Delta F=\int_{A\mathrm{box}} f_{\mathrm{bend}}^{\mathrm{Taylor}}+f_{\mathrm{twist}}^{\mathrm{Taylor}}+f_{\mathrm{splay}}^{\mathrm{Taylor}}+f_{\mathrm{field}}^{\mathrm{Taylor}}+\frac{\Delta\varepsilon E^2}{2}dx\,dy\,dz , \tag{A12}$$

which is explicitly

$$\frac{8\Delta F}{a^2}=(d_xd_yd)\Delta\varepsilon E^2+\frac{K_{33}\pi^2d_xd_y}{d}+\frac{\pi^2}{2}\left[(K_{11}+K_{22})\left[\frac{d_x}{d_y}+\frac{d_y}{d_x}\right]d+\frac{(K_{11}-K_{22})(d_y^2-d_x^2)[(\cos\varphi)^2-(\sin\varphi)^2]}{d_xd_y}\right] . \tag{A13}$$

Now, φ has to be determined such as to minimize the energy. This is done by

(1) $\varphi=0$ if ($K_{11}>K_{22}$ and $d_x>d_y$) or ($K_{11}<K_{22}$ and $d_x<d_y$)

(2) $\varphi=\pi/2$ if ($K_{11}<K_{22}$ and $d_x>d_y$) or ($K_{11}>K_{22}$ and $d_x<d_y$)

(3) φ arbitrary in all other cases.

Accordingly, Eq. (31) becomes either

$$\frac{8\Delta F^{(1)}}{a^2}=d_xd_yd\,\Delta\,\varepsilon E^2+\frac{K_{11}\pi^2d_yd}{d_x}+\frac{K_{22}\pi^2d_xd}{d_y}+\frac{K_{33}\pi^2d_xd_y}{d} \tag{A14}$$

or

$$\frac{8\Delta F^{(2)}}{a^2}=d_x d_y d\,\Delta\varepsilon E^2+\frac{K_{11}\pi^2 d_x d}{d_y}+\frac{K_{22}\pi^2 d_y d}{d_x}+\frac{K_{33}\pi^2 d_x d_y}{d}\ . \tag{A15}$$

Depending on the field strength E, a small distortion of the homeotropic state can either increase or decrease the total energy. The critical field is determined by $F^{\text{delta}}=0$. The two solutions are

$$E^{(1)}_{\text{crit}}=\pi\left[\frac{1}{|\Delta\varepsilon|}\left(\frac{K_1}{d_x^2}+\frac{K_2}{d_y^2}+\frac{K_3}{d^2}\right)\right]^{1/2},\qquad E^{(2)}_{\text{crit}}=\pi\left[\frac{1}{|\Delta\varepsilon|}\left(\frac{K_1}{d_y^2}+\frac{K_2}{d_x^2}+\frac{K_3}{d^2}\right)\right]^{1/2}, \tag{A16}$$

and Eq. (16) follows immediately.

Remember that Eq. (34) is only an approximation if $K_1\neq K_2$. By comparison with numerically obtained threshold values, a deviation of 7% was found when $K_1/K_2=5$. Nevertheless, this calculation provides a qualitative understanding of the new 3D effect.

3. Derivation of the 3D Fréedericksz threshold for the double-twist instability

Since the distortion mode to be considered here, the DT distortion, is spherically symmetric, I assumed a nematic confined to a spherocylinder with radius R and height d. One appropriate ansatz is

$$n=\begin{bmatrix}\sin(-\varphi)\sin[av(r)u(z)]\\ \cos(-\varphi)\sin[av(r)u(z)]\\ \cos[av(r)u(z)]\end{bmatrix}. \tag{A17}$$

Again, a is a small number. With $v(0)=v(R)=0$ and $u(0)=u(d)=0$, this ansatz describes a director field which looks like that in Fig. 7(b). Following the same procedure as in Sec. 2 of this appendix, one obtains the Taylor expansion of the free energy density:

$$2f^{\text{Taylor}}=\Delta\varepsilon E^2+a^2\left|\frac{K_{22}u(z)}{r^2}[v^2(r)+rv'(r)]^2+K_{33}v^2(r)u'^2(z)+\Delta\varepsilon E^2u^2(z)v^2(r)\right|. \tag{A18}$$

The corresponding Euler-Lagrange equation for $v(r)$ is

$$v(r)\left|1+\frac{\Delta\varepsilon E^2r^2}{K_{22}}+\frac{K_{33}r^2u'^2(z)}{K_{22}u^2(z)}\right|-rv'(r)-r^2v''(r)=0\ , \tag{A19}$$

and the Euler-Lagrange equation for $u(z)$ is

$$r^2u''(z)-\frac{K_{22}}{K_{33}}\left|1+\frac{\Delta\varepsilon E^2r^2}{K_{22}}+\frac{r^2v'^2+2rv'(r)}{v(r)}\right|u(z)=0\ . \tag{A20}$$

I could not find a strict solution of this system. As an approximation, however, one can solve Eq. (37) at constant z, and Eq. (38) at constant r. This yields

$$v(r)=J_1\left(\frac{b_0r}{R}\right)\quad\text{and}\quad u(z)=\sin\left(\frac{\pi z}{d}\right). \tag{A21}$$

Here and below, J_n are the Bessel functions of nth order, and b_0 is the first zero of J_1. Fortunately, this approximate solution is a good fit to the director field obtained numerically by the "threshold finder."

Inserting Eq. (39) into Eq. (35) into Eq. (36) yields the energy difference (per volume) to the undistorted state:

$$\frac{\Delta f}{a^2}=K_{22}\left|\frac{\sin\left(\frac{\pi z}{d}\right)}{2rR}\right|^2+\left|b_0rJ_0\left(\frac{b_0r}{R}\right)+2RJ_1\left(\frac{b_0r}{R}\right)-b_0rJ_2\left(\frac{b_0r}{R}\right)\right|^2+K_{33}\left|\frac{\pi}{d}J_1\left(\frac{b_0r}{R}\right)\cos\left(\frac{\pi z}{d}\right)\right|^2+\Delta\varepsilon E^2\left|J_1\left(\frac{b_0r}{R}\right)\sin\left(\frac{\pi z}{d}\right)\right|^2. \tag{A22}$$

The total energy difference is then

$$\frac{\Delta F}{a^2}=\frac{2\pi}{a^2}\int_0^d\int_0^R r(\Delta f)\,dr\,dz=\pi\left|K_{22}Ad+\frac{K_{33}(B\pi)^2R^2}{d}+\Delta\varepsilon E^2BR^2\right|, \tag{A23}$$

where $A=1.190\,82$, $B=0.081\,107\,6$, and $A/B=b_0^2$. At the critical field, $\Delta F=0$ is required, which yields Eq. (17).

[1] F. Lonberg and R. B. Meyer, Phys. Rev. Lett. **55**, 718 (1985).

[2] R. Cohen and M. Luskin, *Nematics: Mathematical and Physical Aspects*, Vol. 332 of *NATO Advanced Study Institute, Series C*, edited by J. F. Coron, F. Helein, and J. M. Ghidaglia (Kluwer Academic, Dordrecht, Netherlands, 1991), pp. 261.

[3] C. Oldano, Phys. Rev. Lett. **56**, 1098 (1986).

[4] J. Deuling, Mol. Cryst. Liq. Cryst. **19**, 123 (1972).
[5] G. Verthoogen and W. H. De Jeu, *Thermotropic Liquid Crystals* (Springer Verlag, Berlin, 1987).
[6] S. Hess, Z. Naturforsch, Teil A **30**, 728 (1975); **31**, 1507 (1975).
[7] A. Kilian and S. Hess, Z. Naturforsch, Teil A **44**, 693 (1989).
[8] D. W. Berreman, Appl. Phys. Lett. **25**, 12 (1974).
[9] W. Greubel, Appl. Phys. Lett. **25**, 5 (1974).
[10] F. Gharadjedaghi and R. Voumard, J. Appl. Phys. **53**, 7306 (1982).

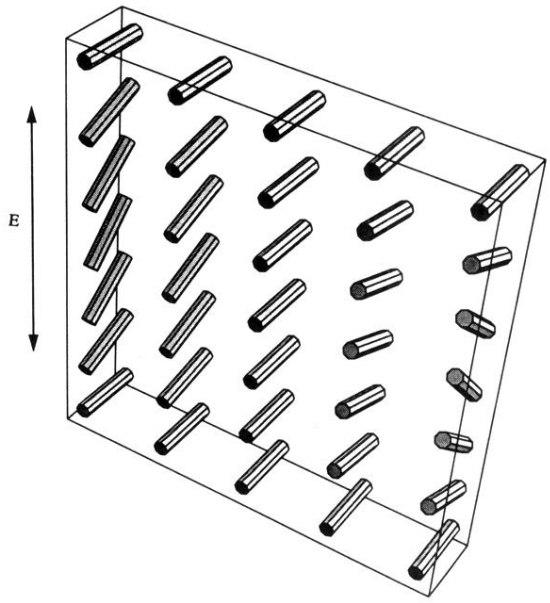

FIG. 1. Periodic bend-splay distortion that occurs for large ratios of K_1/K_2.

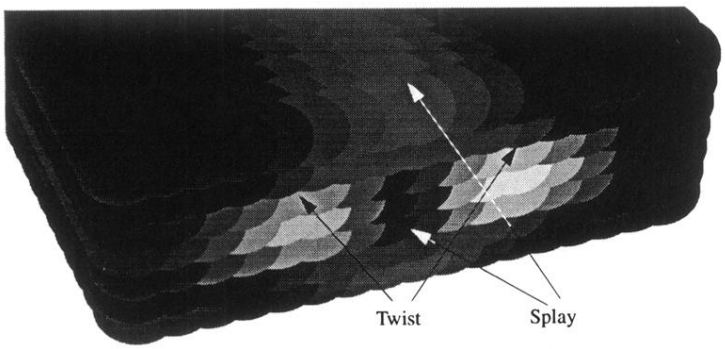

FIG. 5. Spatial distribution of the elastic energies for the splay-twist distortion occurring at a ratio $K_1/K_2=5$.

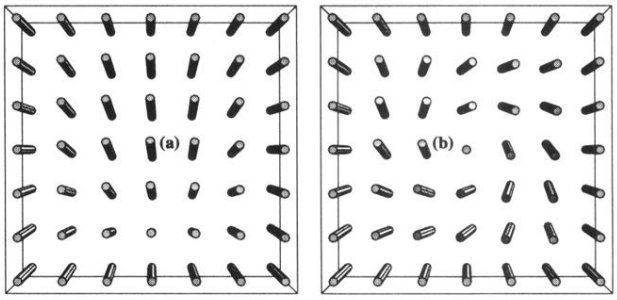

FIG. 7. Top view of the director fields slightly above the threshold (only the center layer is depicted). The small distortion has been amplified by a factor of 10. (a) At $K_1/K_2=1$, the director field exhibits the usual bend-twist-splay instability mode (BTS), that is, it may tilt in one (arbitrary) direction. (b) At $K_1/K_2=7$, the director field is rotationally symmetric, and any radius vector coincides with a twist axis, so that a double-twist distortion (DT) occurs.

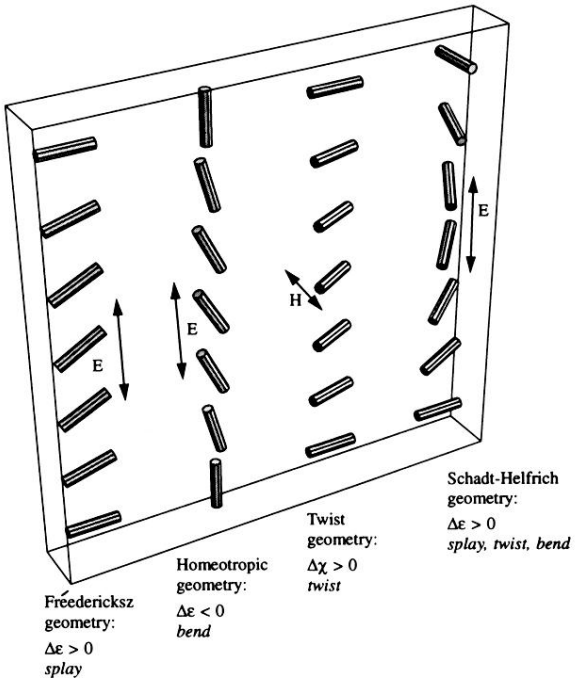

FIG. 9. Distortion modes of some geometries which exhibit Fréedericksz transitions. The double arrow indicates the direction of the applied field.